Detaching the Antiferromagnetic Quantum Critical Point from the Fermi Surface Reconstruction in $YbRh_2Si_2$

Sven Friedemann, Manuel Brando, Philipp Gegenwart[1], Christoph Geibel, Cornelius Krellner, Niels Oeschler, Tanja Westerkamp, Steffen Wirth, and Frank Steglich

A continuous phase transition driven to zero temperature by the application of a non-thermal parameter terminates in a quantum critical point (QCP). At present, two main theoretical approaches are available to describe the antiferromagnetic (AF) QCP in heavy-fermion (HF) systems. The conventional one is based on the quantum generalization of finite temperature phase transitions and reproduces the physical properties in many cases [1-5]. More recent unconventional models introduce an additional energy scale T^* (along with the magnetic one T_N) at which the Kondo effect breaks down, giving rise to more drastic effects [6-8]. YRh_2Si_2 is a prototypical member of a limited group of materials which fall into the latter category [5, 9-11]. In this system, T^* and T_N merge at the magnetic field (H) induced QCP. Here, we study the evolution of $T^*(H)$, $T_N(H)$ and the quantum criticality in $YbRh_2Si_2$ under chemical pressure. Surprisingly, for positive pressure these energy scales intersect whereas negative pressure induces their separation leaving an intermediate spin-liquid type ground state over an extended field range, in contrast to the narrow region expected at a single QCP. This may suggest a new quantum phase arising from the interplay of the Kondo breakdown and the AF QCP.

In HF systems, the Kondo effect leads to the formation of composite quasiparticles of the f and conduction-electron states with largely renormalized masses forming a Landau Fermi liquid (FL) ground state in the paramagnetic regime well below the Kondo temperature T_K. These quasiparticles are assumed to stay intact at the QCP in the conventional models in which magnetic order arises through a spin-density-wave (SDW) instability. However, the observation of magnetic correlations in $CeCu_{5.9}Au_{0.1}$ being of local character [10] prompted a series of theoretical descriptions which discard this basic assumption. Rather, they focus on the breakdown of the Kondo effect which causes the f states to become localised and decoupled from the conduction-band states at the

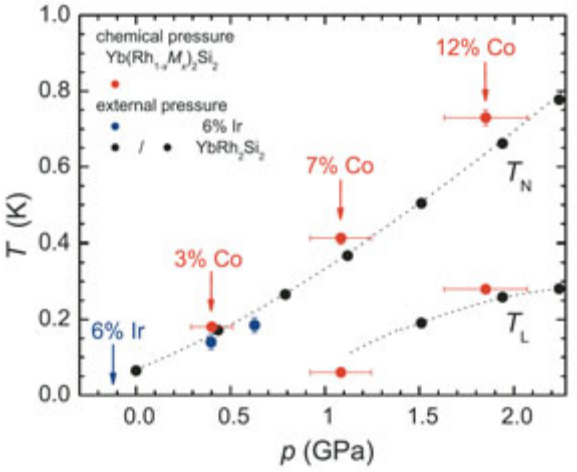

Fig. 1: Equivalence of external and chemical pressure. The Néel temperature T_N of $YbRh_2Si_2$ under pressure is taken from Ref. 18 in good agreement with data from Ref. 19. For pressures above 1.5 GPa a second transition is observed at T_L. The transition temperatures in $Yb(Rh_{1-x}M_x)_2Si_2$ with Ir and Co substitution [20] are plotted on the pressure axis based on the measured lattice parameters and using the bulk modulus of $YbRh_2Si_2$ [21]. The pressure dependence of T_N for 6%Ir was shifted by -0.06 GPa, the chemical pressure introduced by the substitution [22].

QCP where one expects the Fermi surface (FS) to be reconstructed [7]. Consequently, a new energy scale T^* is predicted to exist reflecting the finite temperature crossover of the FS volume. This picture has been scrutinized in tetragonal $YbRh_2Si_2$ ($T_K \approx 25$ K [12]), a stoichiometric and very clean HF metal which appears to be ideally suited for this kind of study [11,12]: AF order sets in at a very low temperature $T_N = 0.07$ K and can easily be suppressed by $\mu_0 H_N = 60$ mT ($H \perp c$, with c the magnetically hard axis). Hall-effect experiments [13] have detected a rapid change of the Hall coefficient along a line $T^*(H)$ with the width of this crossover extrapolating to zero for $T \rightarrow 0$. This was considered as evidence for an abrupt change of the FS volume indicating a correspondence between $T^*(H)$ and the Kondo breakdown energy scale. Subsequent thermodynamic and transport investigations confirmed $T^*(H)$ to be a new energy scale [14].

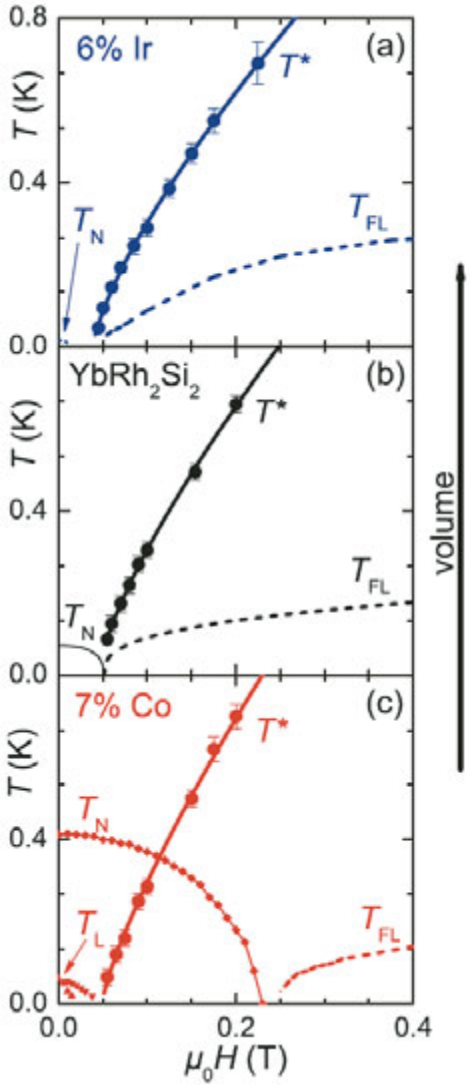

Fig. 2: Evolution of the T-H phase diagram of $YbRh_2Si_2$ under negative and positive chemical pressure. Open circles represent the position of T(H) determined from the maximum of the ac susceptibility $\chi'(T)$. The crossover temperature to the Landau Fermi liquid state, T_{FL}, was deduced from the onset of the quadratic temperature dependence in the electrical resistivity $\rho(T)$. In the phase diagram of $Yb(Rh_{0.94}Ir_{0.06})_2Si_2$ (upper panel) the dotted line renders the phase boundary of the antiferromagnetically ordered state estimated from that of $YbRh_2Si_2$ by scaling both axes with $a = T_N(6\%Ir) / T_N(YbRh_2Si_2) \approx 0.29$. For $Yb(Rh_{0.93}Co_{0.07})_2Si_2$ (lower panel), the Néel temperature T_N was determined from $\rho(T)$. The lower transition at T_L as derived from χ' bifurcates in finite fields. Data for pure $YbRh_2Si_2$ are reproduced from Ref. 14. Lines are guides to the eye.*

In particular, the ac susceptibility $\chi'(T)$ turned out to display a pronounced maximum at T^* which can well be distinguished from the sharp signature at T_N. The magnetoresistance exhibits a step-like crossover similar to the Hall coefficient. In fact, recent calculations for a Kondo lattice predict such a feature for both transport properties [15]. Furthermore, the magnetization shows a smeared kink at $T^*(H)$ between two almost linear regimes with different slopes [14].

The FS reconstruction may also occur away from the AF QCP as observed in $CeIn_3$ and $CeRh_{1-x}Co_xIn_5$ [16,17]. It is therefore very important to understand the interplay between the phenolmena assigned to the Kondo breakdown and the magnetic order. We address this issue by investigating $YbRh_2Si_2$ under positive and negative chemical pressure which was realized by partial isoelectronic substitution of smaller Co or larger Ir for Rh, respectively. The equivalence between external and chemical pressure is suggested from the plots in Fig. 1: The transition temperatures obtained with both methods match very well. In Yb-systems, pressure yields a stabilization of magnetism, in particular an increase of T_N [23]. On the other hand, negative pressure, corresponding to a lattice expansion, reduces T_N.

The *T-H* phase diagrams of $Yb(Rh_{0.94}Ir_{0.06})_2Si_2$ and $Yb(Rh_{0.93}Co_{0.07})_2Si_2$ (labeled 6%Ir and 7%Co in the following) are compared to that of $YbRh_2Si_2$ in Fig. 2. This set emphasizes the evolution of the various energy scales. Firstly, the magnetic one follows the expected pressure dependence: For 6%Ir, T_N is suppressed below 20 mK, whereas in the case of 7%Co T_N is enhanced to 0.41 K. Secondly, the energy scale $T^*(H)$ does virtually not change its position in the *T-H* phase diagram. Consequently, $T^*(H)$ is separated from $T_N(H)$ in 6%Ir, while they intersect in 7%Co. Finally, at fields above the respective critical fields H^* (for 6%Ir) and H_N (for 7%Co), at which $T^*(H)$ and $T_N(H)$ vanish, the FL phase forms below $T_{FL}(H)$.

These findings were mainly deduced from the temperature-dependent ac susceptibility $\chi'(T)$ depicted in Fig. 3. For 6%Ir, no signature of magnetic order is observed as the zero-field curve increases monotonically with decreasing *T*. An antiferromagnetically ordered state is anticipated at even lower temperatures. On the other hand, $\chi'(T)$ of 7%Co exhibits a sharp kink at $T_N = 0.41$ K and a cusp at $T_L = 0.06$ K, the critical temperature of a second, presumably also AF, transition. In external fields, these two transitions are shifted to lower temperatures with the lower one bifurcating (see Fig. 2, lower case). For 6%Ir and 7%Co, a

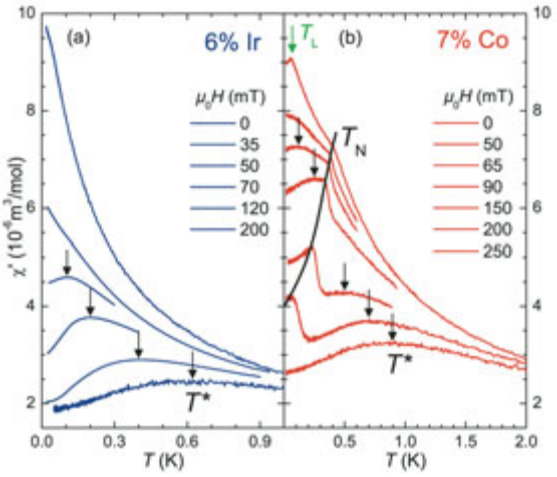

Fig. 3: Signatures of the energy scales T^* (H) and $T_N(H)$ in the susceptibility. Temperature dependent ac susceptibility χ' of $Yb(Rh_{0.94}Ir_{0.06})_2Si_2$ (a) and $Yb(Rh_{0.93}Co_{0.07})_2Si_2$ (b) at selected magnetic fields $H \perp c$. Black arrows indicate the temperatures of the maxima assigned to T^*. For the 7%Co sample the onset of antiferromagnetic ordering in $\chi'(T)$ is marked by the black line. A second transition at T_L is reflected as a peak in χ', marked by a green arrow.

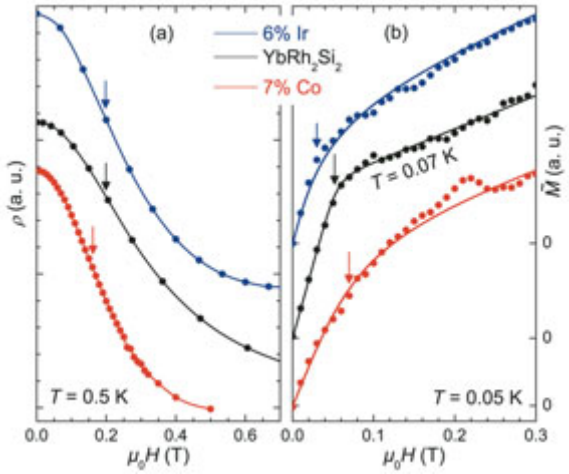

Fig. 4: Signatures of $T^*(H)$ in magnetoresistance and magnetization. Field dependence of (a) magnetoresistance for $Yb(Rh_{0.94}Ir_{0.06})_2Si_2$, $Yb(Rh_{0.93}Co_{0.07})_2Si_2$ and $YbRh_2Si_2$ at 0.5 K and (b) $\tilde{M} = M + \chi' H$ for the former two at 0.05 K. For the case of $YbRh_2Si_2$, the $\tilde{M}$ curve at T_N is shown to avoid an interference of T^* and T_N. In (b) solid lines represent fits of the empirical function $\int_0^H A_1 - (A_1 + A_2) / (1 + (H' / H)^p)\, dH'$ from which the crossover field H_0 (marked by arrows) was obtained [14]. Both the inflection points of the magnetoresistance (also marked) and the $\tilde{M}$-crossover at H_0 are assigned to T^* (H) [14]. The different trend of the crossover field as a function of chemical pressure in magnetoresistance and magnetization is a result of the different temperatures.

maximum in $\chi'(T)$ assigned to $T^*(H)$ is observed above 45 mT and 55 mT, respectively. In an increasing field, this maximum shifts to higher temperatures. Remarkably, for 7%Co the maximum appears both below T_N at small fields, and above T_N at fields of 150 mT and higher. This clearly illustrates that the energy scales, $T_N(H)$ and $T^*(H)$, indeed intersect.

In Fig. 4, we compare the signatures of $T^*(H)$ in magnetoresistance as well as in magnetization for stoichiometric $YbRh_2Si_2$, 7%Co, and 6%Ir. At 0.5 K, the magnetoresistance curves of these three samples exhibit an almost identical, step-like crossover. In particular, the inflection point assigned to $T^*(H)$ [14] is nearly unchanged by chemical pressure resembling the results from susceptibility and magnetization (discussed below). In the case of 7%Co this holds true above T_N, whereas at lower temperatures the inflection point is locked to the AF phase boundary (not shown). The width of the crossover at $T^*(H)$ in magnetoresistance as well as in magnetization appears to follow the unique behavior of $YbRh_2Si_2$ in the temperature range above T_N. For $YbRh_2Si_2$ and 6%Ir, these widths vanish within the experimental resolution for $T \rightarrow 0$, implying a jump at zero temperature [14].

We have analyzed the magnetization M as outlined in Ref. 14 as $\tilde{M} = M + \partial M/\partial H \cdot H = M + \chi' H$. In Fig. 4(b), we focus on data at lowest temperatures, which unambiguously prove the existence of the T^* anomaly also within the AF phase of 7%Co. $\tilde{M}$ (H) exhibits a broadened kink at $T^*(H)$ between two linear regimes with different slopes [14]. In addition to, but clearly distinct from, this kink at $T^*(H)$, a small peak is observed at 220 mT for 7%Co, which is related to the critical field H_N. Therefore, our magnetization and susceptibility results on 7%Co yield striking evidence for the crossover at $T^*(H)$ to also occur inside the AF ordered phase. A re-examination of existing magnetization data [24] confirms this finding for $YbRh_2Si_2$ under external pressure, supporting the equivalence to chemical pressure. In order to check for possible disorder effects, a comprehensive study of $YbRh_2Si_2$ under hydrostatic pressure is in preparation.

Exactly such an intersection of $T_N(H)$ and $T^*(H)$, as observed for 7%Co, was predicted by Si *et al.* [6] for the Kondo lattice in the presence of three dimensional (3D) critical fluctuations. As a result,

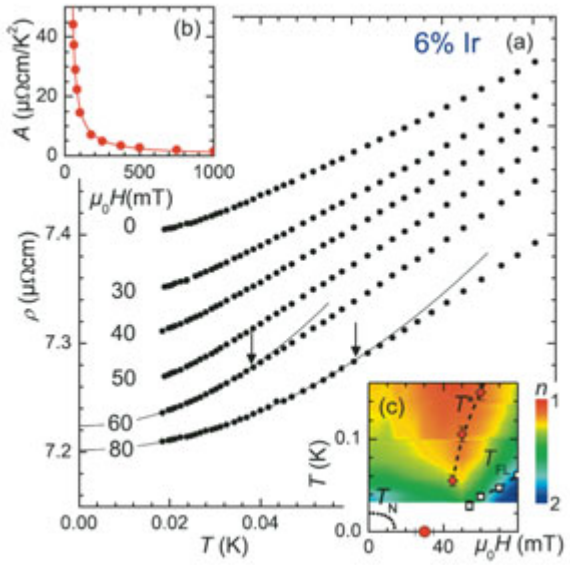

Fig. 5: Signatures of FL and NFL behavior in the temperature dependence of the resistivity of $Yb(Rh_{0.94}Ir_{0.06})_2Si_2$. (a) ρ (T) of 6%Ir at selected magnetic fields. Lines indicate FL behavior, i.e. fits to $\rho(T) = \rho_0 + AT^n$ with n = 2 and ρ_0 the residual resistivity, for temperatures below T_{FL} (marked by arrows). In (b) the field dependence of $A = (\rho(T) - \rho_0) / T^n$ in the FL-regime is shown. The red line corresponds to $A(H) \propto (H - H_c^A)^{-1}$ yielding a critical field of $\mu_0 H_c^A$ = 30(5) mT. (c) Color-coded representation of the resistivity exponent calculated as $n = d\log(\rho(T) - \rho_0) / d\log T$. The energy scales T_N, T^* and T_{FL} are reproduced from Fig. 1(a). The red dot on the abscissa depicts H_c^A.

the AF QCP is expected to be described by the SDW theory. This is well supported by the field dependence of the Néel temperature in the vicinity of H_N (not shown). Moreover, Ref. [6] predicts that critical fluctuations ought to be 2D once $T_N(H)$ and $T^*(H)$ merge at the same QCP, as observed for pure $YbRh_2Si_2$ [13,14]. Note in this respect that – despite equivalent influences of chemical and external pressure on T_N - some slight effect of disorder on the dimensionality of the critical fluctuations cannot be completely ruled out.

We now turn to the interesting case of 6%Ir where, according to our results, the critical fields H_N and H^* appear to become separated from each other (Fig. 2(a)). The resistivity vs. temperature curves measured in various fields are shown in Fig. 5(a). In zero field $\rho(T)$ is quasi-linear below 1 K with a slight upward curvature at the lowest temperatures. In small external fields, this curvature is reduced yielding the steepest curve at 50 mT. At larger fields, a T^2 -dependence is observed (cf. lines in Fig. 5(a)) which indicates that a FL ground state forms below T_{FL}. With increasing field T_{FL} rises. An important finding of this study is that T_{FL} extrapolates to zero at the critical field H^* of the T^* line, rather than at H_N (cf. Fig. 5(c)). Thus, neither the crossover at $T^*(H)$ nor that at $T_{FL}(H)$ seems to be linked to the critical field $\mu_0 H_N \approx 15$ mT of the antiferro-magnetically ordered phase.

The A coefficient in the FL regime, being proportional to the effective quasiparticle-quasiparticle scattering cross section, strongly increases towards low fields (Fig. 5(b)). It follows a $(H - H_c^A)^{-1}$ divergence with a critical field of $\mu_0 H_c^A$ = 30(5) mT being in the vicinity of H^*. This fact provides evidence for the presence of a QCP connected with the vanishing energy scale T^*. Further support for a QCP at H^* stems from the analysis of the resistivity exponent n in $(\rho(T) - \rho_0) \propto T^n$, displayed in Fig. 5(c) as a colored contour plot. The blue region (n = 2) reflects the FL behavior. Deviations from this are ascribed to the quantum criticality [11]: In fact, the red region (n = 1) is clearly linked to T^* and well separated from the critical field of the AF order. To underline that the QCP at H^* cannot be of magnetic origin, we performed χ' measurements on a sample with 17% Ir substitution and, although here no AF order is expected at all, the $T^*(H)$ line is still at the same position in the phase diagram [20]. This suggests a separation of the AF QCP from the Kondo-breakdown QCP. In the intermediate field range, the local f moments are expected to be neither Kondo screened nor antiferromagnetically ordered. This highlights a new metallic "spin-liquid`` (SL)-type ground state that has to be explored in more detail. We note that similar behavior was observed for $Yb_{0.95}La_{0.05}Rh_2Si_2$, where $\rho(T)$ is linear for fields up to 40 mT, and neither a magnetically ordered nor a FL ground state was found [25]. The existence of a SL phase in a Kondo lattice has been speculated [8,26], but the conditions under which it might be realized remain uncertain. Nonetheless, the experimental evidence of such a new, non-magnetic ground state is fascinating and will certainly motivate future experimental and theoretical studies.

In Fig. 6 the evolution of the two different QCPs as a function of Ir/Co substitution is displayed. Here, data for $Yb(Rh_{1-x}M_x)_2Si_2$ with 2.5% Ir and 3% Co have been included. The following main results can be deduced from this figure: (i) The AF state is stabilized through the application of posi-

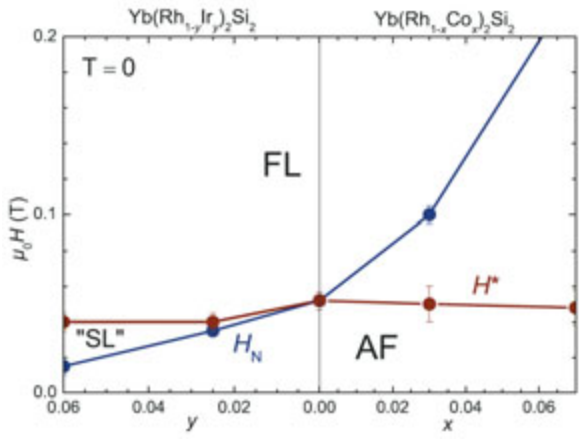

Fig. 6: Experimental phase diagram in the zero temperature limit. The zero-temperature phase diagram depicts the extrapolated critical fields of the various energy scales. The red line represents the critical field of T(H) and the blue line the antiferromagnetic critical field H_N. The region situated between the FL and the AF phase is a phase which resembles a spin liquid.*

tive chemical pressure, as expected. (ii) The position of the suggested breakdown of the Kondo effect manifesting itself as a FS reconstruction depends only weakly on chemical pressure, although the Kondo effect itself is known to be strongly pressure dependent. (iii) For positive pressure, the AF QCP at H_N is located in the regime with intact Kondo screening ($H_N > H^*$) where the SDW theory is expected to be applicable in accordance with our observations. (iv) For negative chemical pressure, on the other hand, H_N is separated from H^* towards lower fields with an intermediate SL-type ground state emerging. Obviously, here, AF order and the FL ground state are not connected by a single QCP, but are separated by a SL, i.e. a NFL range as previously observed in MnSi [27] and, perhaps, in β-$YbAlB_4$ [28,29].

The results and their interpretation presented in this paper pose a formidable challenge for those theories describing a Kondo breakdown near AF QCPs in Kondo lattices. It remains to be explored under which conditions AF ordering and the FS reconstruction may eventually become separated as we have found for $YbRh_2Si_2$ with Ir substitution. The nature of the emerging SL-type ground state will have to be unraveled by future experimental and theoretical studies.

At the same time, it needs to be understood why in pure $YbRh_2Si_2$, the AF QCP is "locked-in" by the Kondo breakdown. In the framework of the local critical scenario a coincidence of the two occurs as a natural consequence of reduced dimensionality of the AF quantum critical fluctuations, whereas the intersection observed in 7%Co is predicted in the 3D case [6].

References

[1] *J. A. Hertz,* Phys. Rev. B **14** (1976) 1165.
[2] *A. J. Millis*, Phys. Rev. B **48**, (1993) 7183.
[3] *T. Moriya and T. Takimoto*, J. Phys. Soc. Jpn. **64** (1995) 960.
[4] *H. v. Löhneysen et al.,* Rev. Mod. Phys. **79** (2007) 1015.
[5] *P. Gegenwart, Q. Si and F. Steglich*, Nature Phys. **4** (2008) 186.
[6] *Q. Si et al.*, Nature **413** (2001) 804.
[7] *P. Coleman et al.,* J. Phys.: Condens. Matter **13** (2001) R723.
[8] *T. Senthil, M. Vojta and S. Sachdev*, Phys. Rev. B **69** (2004) 035111.
[9] *T. Park et al.*, Nature **456** (2008) 366.
[10] *A. Schröder et al.*, Nature **407** (2000) 351.
[11] *J. Custers et al.*, Nature **424** (2003) 524.
[12] *O. Trovarelli et al.*, Phys. Rev. Lett. **85** (2000) 626.
[13] *S. Paschen*, Nature **432** (2004) 881.
[14] *P. Gegenwart et al.*, Science **315** (2007) 969.
[15] *P. Coleman, J. B. Marston and A. J. Schofield*, Phys. Rev. B **72** (2005) 245111.
[16] *N. Harrison et al.*, Phys. Rev. Lett. **99** (2007) 056401.
[17] *S. K. Goh et al.*, Phys. Rev. Lett. **101** (2008) 056402.
[18] *S. Mederle et al.*, J. Phys.: Condens. Matter **14** (2002) 10731.
[19] *G. Knebel et al.*, J. Phys. Soc. Jpn. **75** (2006) 114709.
[20] *T. Westerkamp et al.*, Physica B **403** (2008) 1236.
[21] *J. Plessel et al.*, Phys. Rev. B **67** (2003) 180403.
[22] *M. E. Macovei et al.*, J. Phys.: Condens. Matter **20** (2008) 505205.
[23] *A. V. Goltsev and M. M. Abd-Elmeguid*, Journal of Physics : Condensed Matter **17** (2005) S813.
[24] *Y. Tokiwa et al.*, Phys. Rev. Lett. **94** (2005) 226402.
[25] *F. Weickert et al.*, Physica B **378-380** (2006) 72.
[26] *C. Pépin*, Phys. Rev. B **77** (2008) 245129.
[27] *N. Doiron-Leyraud et al.*, Nature **425** (2003) 595.
[28] *S. Nakatsuji et al.*, Nature Phys. **4** (2008) 603.
[29] *A. H. Nevidomskyy and P. Coleman*, arXiv: 0811.3220v1 [cond-mat.str-el] (2008).

[1] Present address: I. Physikalisches Institut, Georg-August-Universität, 37077 Göttingen, Germany